ChemMedChem

Chemistry Europe
European Chemical Societies Publishing

Accepted Article

Title: Effects of the 5'-Triphosphate Metabolites of Ribavirin, Sofosbuvir, Vidarabine, and Molnupiravir on CTP Synthase. Implications for Repurposing Antiviral Agents Against SARS-CoV-2

Authors: Thomas D. Gillis and Stephen L. Bearne

To be cited as: *ChemMedChem* **2022**, e202200399

Link to VoR: https://doi.org/10.1002/cmdc.202200399

WILEY-VCH

WILEY-VCH

RESEARCH ARTICLE

Effects of the 5′-Triphosphate Metabolites of Ribavirin, Sofosbuvir, Vidarabine, and Molnupiravir on CTP Synthase Catalysis and Filament Formation. Implications for Repurposing of Antiviral Agents Against SARS-CoV-2

Thomas D. Gillis[a] and Stephen L. Bearne*[a],[b]

[a] Dr. S. L. Bearne, T. D. Gillis
Department of Biochemistry & Molecular Biology
Dalhousie University
Halifax, Nova Scotia, Canada, B3H 4R2
E-mail: sbearne@dal.ca

[b] Dr. S. L. Bearne
Department of Chemistry
Dalhousie University
Halifax, Nova Scotia, Canada, B3H 4R2

Supporting information for this article is given via a link at the end of the document.

Abstract: Repurposing of antiviral drugs affords a rapid and effective strategy to develop therapies to counter pandemics such as COVID-19. SARS-CoV-2 replication is closely linked to the metabolism of cytosine-containing nucleotides, especially cytidine-5′-triphosphate (CTP), such that the integrity of the viral genome is highly sensitive to intracellular CTP levels. CTP synthase (CTPS) catalyzes the rate-limiting step for the *de novo* biosynthesis of CTP. Hence, it is of interest to know the effects of the 5′-triphosphate (TP) metabolites of repurposed antiviral agents on CTPS activity. Using *E. coli* CTPS as a model enzyme, we show that ribavirin-5′-TP is a weak allosteric activator of CTPS, while sofosbuvir-5′-TP and adenine-arabinofuranoside-5′-TP are both substrates. β-d-N^4-Hydroxy-cytidine-5′-TP is a weak competitive inhibitor relative to CTP, but induces filament formation by CTPS. Alternatively, sofosbuvir-5′-TP prevented CTP-induced filament formation. These results reveal the underlying potential for repurposed antivirals to affect the activity of a critical pyrimidine nucleotide biosynthetic enzyme.

Introduction

With the advent of the pandemic of coronavirus disease in 2019 (COVID-19), caused by severe acute respiratory syndrome coronavirus 2 (SARS-CoV-2),[1] it has become clear that there is an urgent need to develop broad spectrum therapeutic approaches to combat pandemics.[2] While vaccines offer an effective approach to prevent many viral infections, their development is laborious and requires long lead times. In the absence of a vaccine, prophylactic use of small molecule antiviral agents offers a promising alternative, especially to protect vulnerable and at-risk populations. Drug repurposing affords a strategy for identifying new uses for approved or investigational drugs in a cost-effective and timely manner when initially faced with no treatment options for a disease, as was the case with COVID-19.[3] Efforts have focused on assessing the efficacy of known broad spectrum antiviral compounds,[4] particularly remdesivir (GS-5734) [5] and molnupiravir (EIDD-2801 or MK-4482).[6] These nucleoside analogues are delivered as prodrugs and subsequently metabolized to their corresponding active 5′-triphosphate (5′-TP) by the action of kinases. Remdesivir-5′-TP directly inhibits the coronavirus RNA-dependent RNA polymerase (RdRp).[7] Competition with endogenous nucleotide substrates for the viral RdRp,[8] which incorporates the analogue into the nascent viral RNA, leads to chain-termination. On the other hand, the 5′-TP metabolite of molnupiravir acts as a mutagen through RNA mutagenesis mediated by the template strand.[9]

Other synergistic approaches to antiviral therapies beyond the direct inhibition of the RdRp of SARS-CoV-2, may also be considered. One such approach is to limit the nucleotide pools to starve the viral replication machinery. Recently, suppression of pyrimidine biosynthesis by inhibition of dihydroorotate dehydrogenase has been shown to restore the antiviral inflammatory response and reduce viral yield upon SARS-CoV-2 infection.[10] Danchin and co-workers postulated that SARS-CoV-2 replication is closely linked to the metabolism of cytosine-containing nucleotides, especially cytidine-5′-TP (CTP).[11] Consequently, the integrity of the viral genome would be highly sensitive to intracellular CTP pool levels. CTP plays an integral role in crucial metabolic steps contributing to the manufacture of functional SARS-CoV-2 viral particles.[11c] As well as being one of the four nucleotide precursors required for biosynthesis of the viral genome,[12] it is required for synthesis of the liponucleotide precursors of the viral envelope,[13] for the biosynthesis of the 3′-OH-CCA terminal end of human tRNAs via a CTP-dependent nucleotidyltransferase (CCAse),[14] and for post-translational glycosylation of viral proteins (e.g., the spike protein) via the endoplasmic reticulum, which requires dolichyl-phosphate formed through the action of a CTP-dependent dolichol kinase.[15] Furthermore, CTP is converted into the antiviral agent 3-deoxy-3,4-didehydro-CTP (ddhCTP) by the enzyme viperin as part of the innate immune response.[16]

The sole route for the *de novo* biosynthesis of cytosine in human host cells is through the adenosine-5′-TP (ATP)-dependent conversion of uridine-5′-TP (UTP) to CTP catalyzed by CTP synthase (CTPS),[17] utilizing glutamine (Gln, *in vivo* substrate) or ammonia (NH_3) as the source of nitrogen (**Scheme 1**). The enzyme requires Mg^{2+} ion[18] and is regulated in a complex

fashion by several nucleotide effectors. The substrates ATP and UTP activate the enzyme with positive cooperativity[19] and act synergistically to promote tetramerization of the enzyme to its active form.[19c] The product, CTP, acts as a feedback inhibitor,[19a] and promotes both tetramerization of the enzyme[20] and polymerization of *E. coli* CTPS (*Ec*CTPs) into inactive filaments.[21] On the other hand, human CTPS1 forms substrate-bound filaments,[21c] while human CTPS2[22] and *Drosophila* CTPS[23] can form either substrate- or product-bound filaments. Finally, GTP is a positive allosteric effector for Gln-dependent CTP formation, stimulating both Gln hydrolysis at the C-terminal glutamine amide transfer domain and the subsequent translocation of ammonia to the N-terminal synthase domain, where CTP is generated from UTP.[24]

$$\mathrm{ATP + UTP + Gln + H_2O \xrightarrow[Mg^{2+},\ GTP]{CTPS} ADP + CTP + Glu + P_i}$$

$$\mathrm{ATP + UTP + NH_3 \xrightarrow[Mg^{2+}]{CTPS} ADP + CTP + P_i}$$

Scheme 1. CTP-forming reactions catalyzed by CTP synthase.

CTPS is a recognized target for the development of antiviral agents (*e.g.*, cyclopentenylcytosine-5′-triphosphate[25]).[25a,26] The ability of nucleotide-based CTPS inhibitors to act as antiviral agents and to augment the effects of other antiviral agents,[27] suggests that such inhibitors may be valuable drug candidates for the treatment of COVID-19. Inhibition of CTPS activity could potentiate the effect of antiviral therapies targeting coronavirus infections by reduction of intracellular CTP pools, thereby increasing the likelihood of incorporation of nucleotide analogues. Indeed, remdesivir treatment of human bronchial epithelial cells has been shown to induce a marked disequilibrium between CTP and CMP.[28] Exacerbation of this imbalance in cytosine nucleotide pools with an inhibitor of CTPS may enhance the efficacy of remdesivir. Surprisingly, the effect of many antivirals on CTPS activity have not been examined. Consequently, we sought to explore the effects of several antiviral nucleotide analogues on the activity of CTPS and its ability to form filaments. For these studies, we employed recombinant *Ec*CTPS as a model enzyme since the two human CTPS variants and *Ec*CTPS exhibit high conservation of functionally and structurally important residues and have few insertion/deletion differences.[21c,29] Herein we report the effects of ribavirin-5′-TP (RBV-TP), sofosbuvir-5′-TP (SFU-TP, PSI-7409), adenine-arabinofuranoside-5′-TP (ara-ATP or vidarabine-5′-TP), and β-D-N^4-hydroxycytidine-5′-TP (N^4-OH-CTP, the active metabolite of molnupiravir) on the activity of *Ec*CTPS. While N^4-OH-CTP proved to be a weak inhibitor of CTPS, surprisingly, SFU-TP and ara-ATP were substrates and RBV-TP was an allosteric activator.

Results and Discussion

Effects of ribavirin-5′-TP on *Ec*CTPS activity

Ribavirin is a broad-spectrum antiviral drug wherein the carboxamide moiety of the pseudobase serves as a structural mimic of guanosine and inosine.[30] *In silico* docking studies suggested that RBV-TP would be bound by the SARS-CoV-2 RdRp.[31] Ribavirin appears to be somewhat efficacious as a treatment for COVID-19 in combination with other antiviral agents or with interferon.[32] Ribavirin's antiviral effects can arise through several mechanisms, including inhibition of RNA capping activity, immunomodulatory effects, inhibition of viral polymerases, and increased mutational frequency due its incorporation into the RNA genome during virus replication.[33] *In vivo*, phosphorylation leads to the 5′-monophosphate, 5′-diphosphate, and 5′-TP, with the latter often being the major metabolite.[34] Ribavirin-5′-monophosphate acts as a competitive inhibitor of human inosine-5′-monophosphate dehydrogenase (IMPDH) with respect to GMP,[35] leading to depletion of the intracellular pools of GTP, which contributes indirectly to ribavirin's antiviral activity.[33,36] For example, cultured Madin Darby Canine Kidney (MDCK) cells infected with A/WSN-strain influenza virus reduce the GTP concentration ~50%, in the presence of RBV (100 μM).[36] Interestingly, the intracellular CTP and UTP pools typically increase with ribavirin treatment.[34a,37] (See Table 1 for typical intracellular concentrations of ribonucleoside-5′-TPs.) The concomitant elevation of the CTP pools is unexpected considering that GTP is an allosteric activator of CTPS-catalyzed Gln-dependent CTP formation.[24e] Consequently, we assessed the direct effect of RBV-TP on *Ec*CTPS activity.

Interestingly, RBV-TP served as an allosteric activator similar to GTP (**Fig. 1**). The k_{act} values accompanying activation by GTP and RBV-TP were 9.2 s^{-1} and 13.8 s^{-1}, respectively (**Table 1**). While the k_{act} values were similar, there was a marked increase in the K_A value for RBV-TP (2.44 mM) relative to the K_A value observed for GTP (0.068 mM). Our observation that RBV-TP activates *Ec*CTPS-catalyzed Gln-dependent CTP formation is surprising because the structural requirements for activation are quite stringent, with O6 of GTP being required for activation.[38] Previously, we demonstrated that inosine-5′-TP (ITP) also acts as an allosteric activator, but was bound weakly by the enzyme with a K_A value of 2.9 mM, indicating that the 2-NH_2 group contributes significantly to binding.[38] Consequently, the carboxamide group on the pseudobase of RBV-TP is able to mimic the interaction of O6 with *Ec*CTPS to afford activation, but the missing part of the purine structure diminished the binding affinity similar to ITP.

Because of the ability of nucleotides to induce or reverse filament formation by CTPS,[21c,22-23,39] we examined the effect of RBV-TP on filament formation. Neither GTP nor RBV-TP were capable of inducing *Ec*CTPS filaments alone (**Fig. S1**). Additionally, no distinct differences in filament abundance or length were observed with *Ec*CTPS that had been incubated with CTP, CTP and GTP, or CTP and RBV-TP, indicating that RBV-TP has no apparent effect on filament formation by *Ec*CTPS.

Considering that the concentration of RBV-TP in the red blood cells and bronchoalveolar lavages from patients with respiratory syncytial virus were 313 μM and 514 μM, respectively,[40] it is possible that RBV-TP could replace GTP as a weak allosteric activator of CTPS, thereby furnishing a mechanism by which CTPS can remain active. Although the overall efficiency of activation (k_{act}/K_A) by RBV-TP is ~24-fold less than that of GTP, the allosteric activation of *Ec*CTPS by RBV-TP suggests a mechanism for the continued production of CTP despite the depletion of the GTP pools arising from the inhibition of IMPDH by ribavirin-5′-monophosphate upon ribavirin treatment.[34a,37]

Table 1. Kinetic parameters for *Ec*CTPS-catalyzed Gln-dependent and NH_3-depenent CTP formation

	Gln-dependent CTP formation				NH_3-dependent CTP formation			
varied ligand	K_m or $[S]_{0.5}$[a] or K_A[b] (mM)	k_{cat} or k_{act}[c] (s^{-1})	k_{cat}/K_m, $k_{cat}/[S]_{0.5}$[d], or k_{act}/K_A[e] (s^{-1} mM^{-1})	n]	K_m or $[S]_{0.5}$[a] (mM)	k_{cat} (s^{-1})	k_{cat}/K_m or $k_{cat}/[S]_{0.5}$[d] (s^{-1} mM^{-1})	n
L-Gln[f]	0.25 ± 0.04	10.6 ± 1.1	42.4 ± 8.1	–	–	–	–	–
L-Gln[g]	0.32 ± 0.03	1.21 ± 0.03	3.78 ± 0.37	–	–	–	–	–
NH_3	–	–	–	–	1.72 ± 0.25	10.8 ± 1.7	6.3 ± 1.4	–
ATP	0.21 ± 0.02[a]	11.6 ± 0.6	55.2 ± 6.0[d]	1.18 ± 0.01	0.57 ± 0.03[a]	8.0 ± 0.1	14.0 ± 0.8[d]	3.0 ± 0.5
UTP	0.200 ± 0.004[a]	8.4 ± 0.1	42.5 ± 1.0[d]	2.17 ± 0.18	0.77 ± 0.06[a]	8.1 ± 0.3	10.56 ± 0.86[d]	1.6 ± 0.1
GTP	0.068 ± 0.019[b] K_{inhib} = 0.55 ± 0.05 mM	9.2 ± 1.5[c]	135 ± 44[e]	3.1 ± 0.9	–	–	–	–
RBV-TP	2.44 ± 0.92[b]	13.8 ± 2.6[c]	5.6 ± 2.4[e]	–	–	–	–	–
SFU-TP	0.20 ± 0.01[a]	1.35 ± 0.03	6.75 ± 0.37[d]	1.09 ± 0.14	–	–	–	–
ara-ATP	0.14 ± 0.02[a]	3.1 ± 0.5	22.1 ± 4.8[d]	1.2 ± 0.1	0.60 ± 0.19[a]	1.5 ± 0.3	2.49 ± 0.68[d]	1.4 ± 0.3

[a] $[S]_{0.5}$ is the nucleotide concentration that yields half-maximal velocity. For comparison, the intracellular pool sizes of ribonucleoside-5′-TPs in either uninfected or influenza A virus-infected MDCK cells are 0.28 – 0.59 mM CTP, 0.96 – 1.6 mM UTP, 6.5 – 7.8 mM ATP, and 1.1 – 1.4 mM GTP,[41] and average values in dividing and resting mammalian cells are 0.28 mM and 0.083 mM CTP, 0.57 mM and 0.23 mM UTP, 3.2 mM and 2.5 mM ATP, and 0.47 mM and 0.23 mM GTP, respectively;[42] [b] K_A value; [c] k_{act} value; [d] $k_{cat}/[S]_{0.5}$ value; [e] k_{act}/K_A value; [f] [ATP] = [UTP] = 1.0 mM; [g] [ATP] = [SFU-TP] = 1.0 mM.

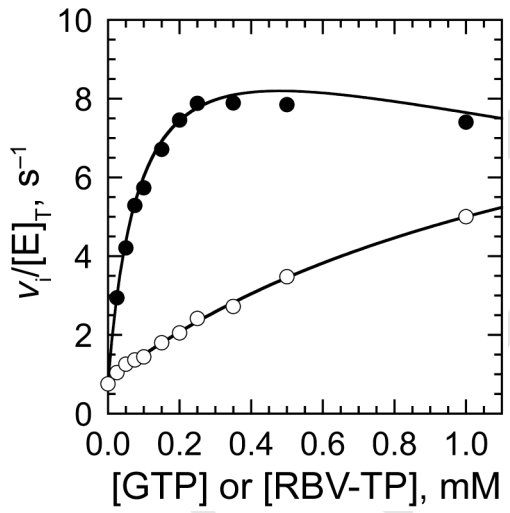

Figure 1. Kinetic characterization of GTP and RBV-TP as allosteric activators of CTPS. Representative plot of the initial velocities of GTP-dependent (●) and RBV-TP-dependent (○) *Ec*CTPS-catalyzed Gln-dependent CTP formation as a function of ligand concentration are shown. The concentration of *Ec*CTPS was 4.7 μg/mL and other substrates were at saturating concentrations. The curves shown for the GTP-dependent and RBV-TP-dependent activation are fits of eqns. 3 and 4 to the steady-state kinetic data, respectively. The k_o value was 0.80 ± 0.05 s^{-1}. The values of k_{act}, K_A, K_{inhib}, and n are summarized in **Table 1**.

Effects of sofosbuvir-5′-TP on *Ec*CTPS activity

SARS-CoV-2 and hepatitis C virus (HCV) are both positive-sense single-stranded RNA viruses requiring an RdRp for genome replication and transcription. Since the amino acid sequence at the active site is highly conserved among such RdRps, it was hypothesized that nucleotide analogues used to treat HCV infections, such as sofosbuvir, might also be effective against COVID-19.[31,43] *In silico* docking studies suggested that the SARS-CoV-2 RdRp would bind SFU-TP.[31] Indeed, SFU-TP is incorporated into RNA by the highly error-prone SARS-CoV-2 RdRp, but not by a host-like high-fidelity DNA polymerase, terminating extension due to its bulky 2′-methyl group.[43b,44] However, other studies have shown that SFU-TP does not inhibit SARS-CoV-2 RdRp[32d,45] or markedly inhibit SARS-CoV-2-induced cytopathic effects,[46] which casts doubt on the utility of sofosbuvir as a treatment for COVID-19.[47]

Because of the attention focused on sofosbuvir, as well as its current use as an anti-HCV drug,[48] we explored the effect of SFU-TP on CTPS activity and found that SFU-TP was a substrate for Gln-dependent *Ec*CTPS-catalyzed amination (**Fig. 2**). While *Ec*CTPS exhibited the same binding affinities for UTP and SFU-TP ($[S]_{0.5}$ ≈ 0.2 mM), the k_{cat} value for Gln-dependent amination of SFU-TP was ~6-fold lower than that for the reaction with UTP (**Table 1**).

To confirm that *Ec*CTPS-catalyzed amination of SFU-TP, we examined the *Ec*CTPS-catalyzed NH_3-dependent amination of SFU-TP by following the depletion of SFU-TP and appearance of 4-NH_2-SFU-TP using mass spectrometry (**Fig. 3**). Conversion of the SFU-TP to the aminated product was clearly visible during the

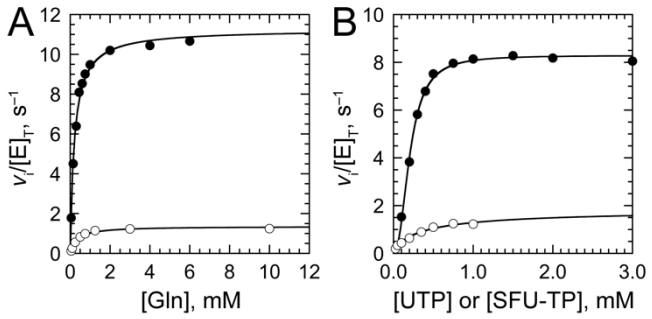

Figure 2. Kinetic characterization of SFU-TP as a substrate of *Ec*CTPS. Representative plots of the initial velocities of Gln-dependent *Ec*CTPS-catalyzed CTP formation at a fixed concentration of UTP (●) or STP (○) (1.0 mM each) and varying the concentrations of Gln (0.05 – 10.00 mM) (**A**) and at a fixed concentrations of Gln (6.0 mM) and ATP (1.0 mM), and varying concentrations of UTP (●) or STP (○) (0.1 – 3.0 mM and 0.025 – 1.000 mM, respectively) (**B**). All other substrates were at saturating conditions. The concentrations of *Ec*CTPS were 6.3 μg/mL and 3.8 μg/mL when UTP and STP were at saturating conditions, respectively (**A**), and 7.6 μg/mL and 3.8 μg/mL when UTP and STP were the variable substrates, respectively (**B**). The curves shown are fits of eqns. 1 (**A**) and 2 (**B**) to the initial velocity data. The corresponding kinetic parameters are summarized in **Table 1**.

time course with the rate of turnover obeying the integrated Michaelis-Menten equation.

Previously, UTP had been shown to reduce the formation of filaments by *Ec*CTPS using transmission electron microscopy (TEM).[21c,39c] SFU-TP also reduced formation of *Ec*CTPS filaments in the presence of CTP (**Fig. 4**), although not as efficiently as previously reported for UTP. Upon increasing the concentration of SFU-TP to ~5 mM, there was a marked decrease in filament abundance. The ability of SFU-TP to reduce filament formation, along with the utilization of SFU-TP as a substrate, is consistent with SFU-TP binding at the overlapping UTP- and CTP-binding sites[29b] and displacing CTP. Thus, SFU-TP can replace UTP as a substrate for *Ec*CTPS, albeit less efficient, and prevent CTP-dependent filament formation by the enzyme. However, it is unlikely that SFU-TP would play a significant role as a substitute for UTP, considering, for example, that in the liver tissue of hepatitis C-infected patients with hepatocarcinoma treated with sofosbuvir (400 mg/day), the median intracellular SFU-TP concentration was only ~5 μM, ranging as high as ~65 μM.[49]

Effects of adenine-arabinofuranoside-5′-TP on *Ec*CTPS activity

In silico screening and molecular dynamics suggested that Ara-A (vidarabine) could inhibit the interaction between the SARS-CoV-2 spike protein S1 receptor binding domain and the ACE2 receptor.[50] Similarly, ara-A was identified through deep learning-based screening as a potential drug to target the 3C-like protease of SARS-CoV-2.[51] Consequently, we examined the effect of the 5′-TP metabolite of ara-A (ara-ATP) on *Ec*CTPS activity.

Ara-ATP served as a substrate for both Gln-dependent and NH_3-dependent *Ec*CTPS-catalyzed CTP formation (**Fig. 5**). The ability of ara-ATP to replace ATP as a substrate for *Ec*CTPS has not previously been recognized. Interestingly, the $k_{cat}/[S]_{0.5}$ value for ara-ATP was ~2.5-fold less than that of ATP for Gln-dependent CTP formation; however, ara-ATP was a much less efficient substrate for NH_3-dependent CTP formation by ~5.5-fold, relative

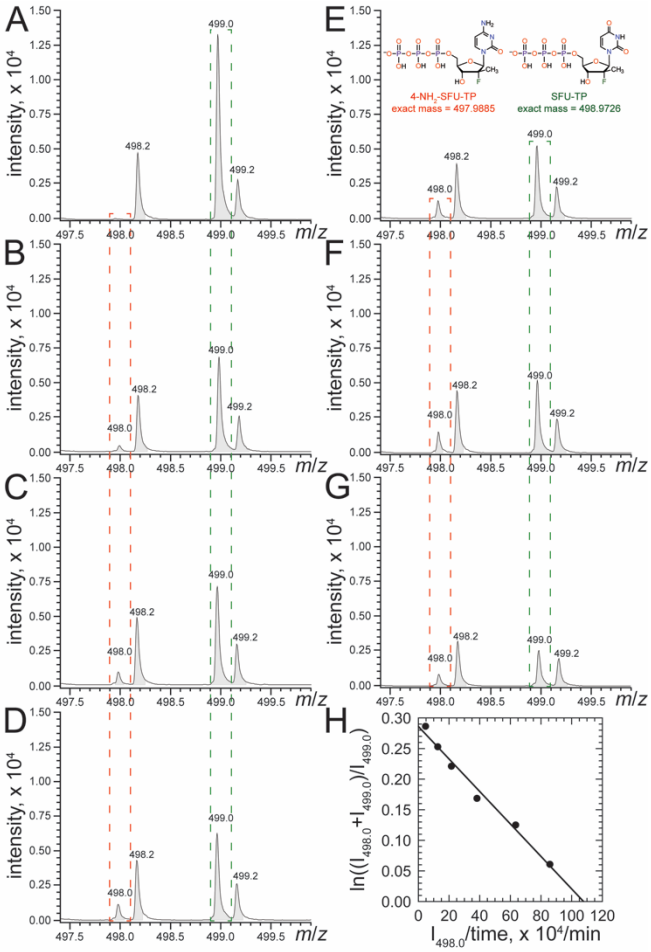

Figure 3. Mass spectral analysis of the *Ec*CTPS-catalyzed NH_3-dependent amination of SFU-TP to form 4-NH_2-SFU-TP. LRESI-MS obtained at 0 (**A**), 5 (**B**), 15 (**C**), 30 (**D**), 60 (**E**), 120 (**F**), and 180 (**G**) min are shown for the reaction of SFU-TP (2.0 mM) with NH_4Cl (150 mM) catalyzed by *Ec*CTPS (0.5 μM) in the presence of ATP (1.0 mM). Plotting the intensity of ions observed with *m/z* values of 498.0 (*i.e.*, 4-NH_2-SFU-TP) and 499.0 (*i.e.*, SFU-TP) revealed that the conversion obeyed the integrated Michaelis-Menten equation (**H**).[52] The red and green dashed boxes indicate the signals corresponding to 4-NH_2-SFU-TP and SFU-TP, respectively.

to ATP. Structural studies by Baldwin and co-workers had revealed that the ribose 2′- and 3′-OH groups have no direct protein contacts in the *Ec*CTPS complex with ADP (although they are near Lys 306 and Asp 303, respectively),[29b] which along with the observation that ATP and dATP were equally effective co-substrates with UTP, led them to conclude that 2′-OH recognition is not important. However, kinetic studies on the K306A variant suggested that Lys 306 plays a role in bringing about the conformational changes that mediate interactions between the ATP-binding site and the UTP-binding site, as well as the glutamine amide transfer domain.[53] The weaker binding of ara-ATP, relative to ATP, reveals that *Ec*CTPS is sensitive the stereochemistry at the 2′-position likely due to unfavorable steric interactions between the *arabino*-2′-OH group and the side chain of Ile 20. In varicella-zoster virus-infected human foreskin fibroblasts, the concentration of ara-ATP is about 4-fold lower than the concentration of ATP, which suggests that while our observations suggest that ara-ATP could assist in maintaining the

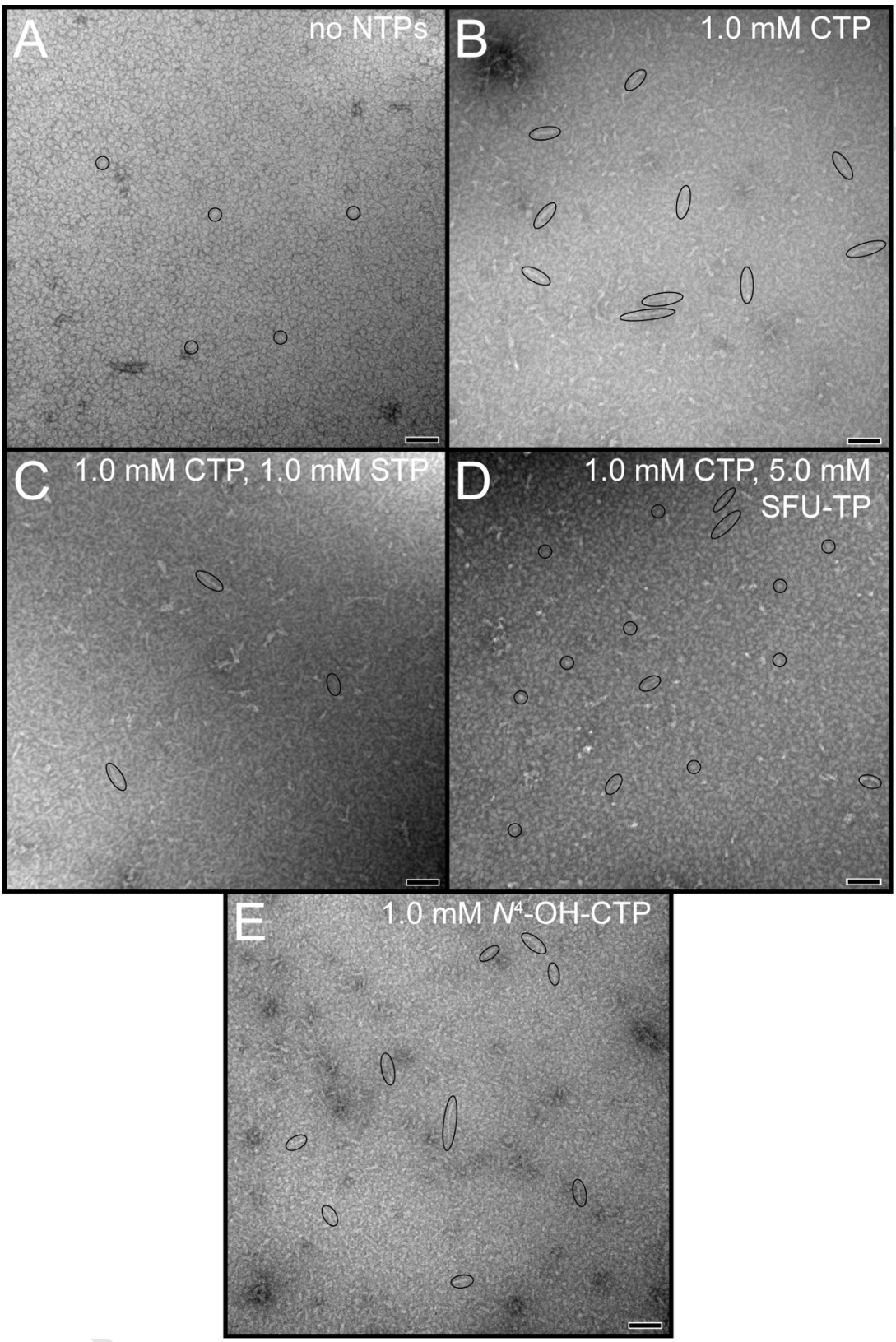

Figure 4. Effect of SFU-TP and N^4-OH-CTP on filament formation by *Ec*CTPS. Representative transmission electron micrographs of *Ec*CTPS in the absence of nucleotides (**A**) and in the presence of CTP (1.0 mM) with either 0 (**B**), 1.0 mM (**C**), or 5.0 mM (**D**) SFU-TP present. Increasing the concentration of SFU-TP causes a marked reduction in the presence of CTP-induced *Ec*CTPS filaments. Like CTP (**B**), N^4-OH-CTP (1.0 mM) induced filament formation by *Ec*CTPS (**E**). Circles and ovals are shown to highlight the appearance of representative non-filamentous structures (possibly protein aggregates) and filaments, respectively. The scale bars correspond to a distance of 100 nm.

intracellular CTP pools when employed as an antiviral agent, the effect may be minimal.

Effects of β-D-N^4-hydroxycytidine-5′-TP on *Ec*CTPS activity

The cytidine analogue β-D-N^4-hydroxycytidine (NHC, which as its isopropyl-ester prodrug is known as molnupiravir or EIDD-2801) exhibits antiviral activity against multiple coronaviruses, including SARS-CoV-2.[9d,45,54]

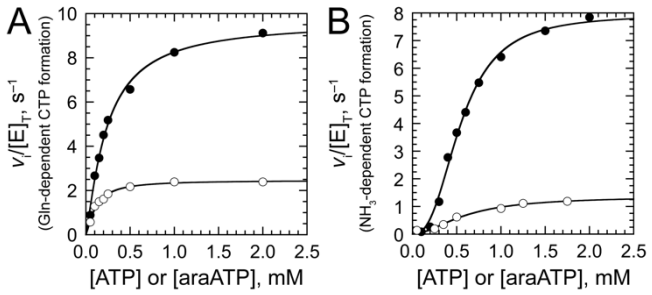

Figure 5. Kinetic characterization of ara-ATP as a substrate of *Ec*CTPS. Representative plots of the initial velocities of *Ec*CTPS-catalyzed Gln-dependent (**A**) and NH_3-dependent (**B**) CTP formation as a function of the concentration of ATP (●) and ara-ATP (○) are shown. Enzyme concentration ranged between 4.7 and 7.6 μg/mL and all other substrates were at saturating concentrations. The curves shown in both panels are fits of eqn. 2 to the steady-state kinetic data. The corresponding kinetic parameters are summarized in **Table 1**.

The active 5′-TP form of molnupiravir (*i.e.*, N^4-OH-CTP) acts as a mutagen[9a,9b,9d,9e,55] causing the RdRp-dependent incorporation of either G or A into RNA products that escape proofreading.[9c,9e,56] Consequently, we tested the effect of N^4-OH-CTP on *Ec*CTPS activity and filament formation.

N^4-OH-CTP was prepared by the reaction of CTP with hydroxylamine, followed by purification using weak anion-exchange chromatography (**Figs. S2-S7**) similar to the protocol described by Painter *et al*.[57] Product formation was confirmed by NMR spectra (**Figs. S8** and **S9**) and MS data (**Fig. S10**), and the product was shown to be pure by reversed-phase HPLC analysis (**Fig. S11**). We determined the IC_{50} values for the inhibition of *Ec*CTPS by CTP and N^4-OH-CTP at two fixed concentrations of UTP (50 and 200 μM) with Gln as the nitrogen source (**Fig. S12**). Comparison of the IC_{50} values revealed that N^4-OH-CTP was a weak inhibitor of *Ec*CTPS, relative to CTP (**Table 2**).

We then investigated the mode of inhibition and determined the value of the inhibition constant (K_i) of both CTP and N^4-OH-CTP (**Fig. 6**). In accord with previous results,[58] CTP was a competitive inhibitor of *Ec*CTPS with respect to UTP. Similarly, N^4-OH-CTP was also a competitive inhibitor of *Ec*CTPS with respect to UTP, albeit binding with an affinity that was 7.7-fold weaker than CTP (**Table 2**). Given the ability of CTP to induce filament formation by *Ec*CTPS,[21b,39c] we investigated the ability of N^4-OH-CTP to induce filament formation. Indeed, N^4-OH-CTP (1.0 mM) was able to induce the formation of *Ec*CTPS filaments that were similar in size and abundance to those induced in the presence of CTP (**Fig. 4,** *cf*. panels B and E).

Table 2. Inhibition of *Ec*CTPS-catalyzed Gln-dependent CTP formation by CTP and N^4-OH-CTP.

inhibitor	[UTP] = 50 μM		[UTP] = 200 μM		K_i, μM
	IC_{50}, μM	*n*	IC_{50}, μM	*n*	
CTP	107 ± 4	1.6 ± 0.1	234 ± 21	1.6 ± 0.1	108 ± 29
N^4-OH-CTP	1112 ± 48	1.7 ± 0.2	1461 ± 44	1.5 ± 0.4	831 ± 79[a]

[a] The intersection of the lines on the Lineweaver-Burk plot appears slightly to the left of the y-axis (**Fig. 6E**). Treating the inhibition as linear mixed-type yields an additional weak binding constant (K_{iint}) of > ~28 mM for the interaction of N^4-OH-CTP with the enzyme-substrate complex.

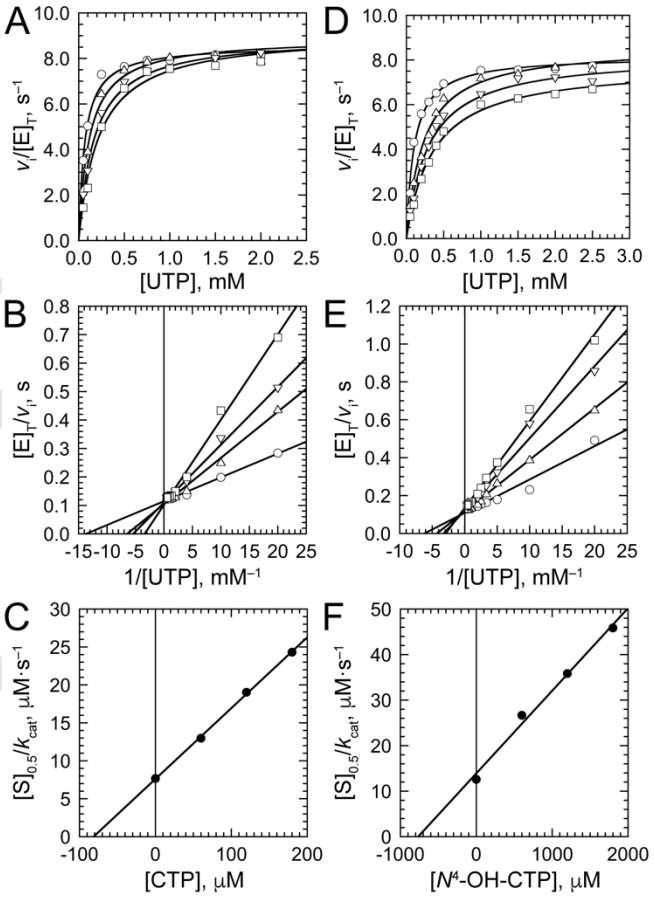

Figure 6. Competitive inhibition of *Ec*CTPS by CTP and N^4-OH-CTP. Representative Michaelis-Menten plots (**A**, **D**) and Lineweaver-Burk plots (**B**, **E**) showing the competitive inhibition of *Ec*CTPS-catalyzed Gln-dependent CTP formation by CTP (**A**, **B**) and N^4-OH-CTP (**D**, **E**) with respect to UTP as the variable substrate are shown. The concentrations of CTP were 0.00 (○), 0.06 (△), 0.12 (▽), and 0.18 (□) mM and the concentrations of N^4-OH-CTP were 0.00 (○), 0.60 (△), 1.20 (▽), and 1.80 (□) mM. The concentrations of *Ec*CTPS were 5.0 μg/mL and 3.9 μg/mL when CTP and N^4-OH-CTP were assayed as inhibitors, respectively. Representative replots of the apparent $[S]_{0.5}/k_{cat}$ values (obtained from direct fits of eqn. 2 with n = 1 to the initial velocity data) as a function of the concentrations of CTP (**C**) and N^4-OH-CTP (**F**) are shown. The inhibition constants (K_i) are given in **Table 2**.

Thus, the active metabolite of NHC weakly inhibits *Ec*CTPS activity and effects filament assembly. The ability of N^4-OH-CTP to inhibit *Ec*CTPS has not previously been recognized. Overall, these observations suggest that N^4-OH-CTP, in addition to

causing mutation in the viral genome,[59] could also reduce the intracellular CTP pools. However, the latter effect may be weak, considering that the concentration of N^4-OH-CTP in peripheral blood mononuclear cells has been shown to reach concentrations of 60 – 85 μM in patients receiving a single oral dose of 1600 mg,[60] i.e., ~20-fold below the IC_{50} values reported in **Table 2**.

Conclusions

Since repurposing of small molecule antiviral drugs can afford a rapid and effective strategy to develop therapies to counter pandemics such as COVID-19,[2] it is important to assess potential synergistic or detrimental effects that such drugs might have against alternative enzyme targets. Indeed, the close link between SARS-CoV-2 replication and the metabolism of cytosine-containing nucleotides, especially CTP, and the sensitivity of the viral genome to intracellular CTP levels,[11] necessitates exploration of the effect of the active metabolites of antiviral drugs on the activity and regulation of CTPS. Surprisingly, the effect of the 5′-TP metabolites of many antivirals on CTPS activity have not been examined. Consequently, we employed *Ec*CTPS as a model enzyme to explore the effects of RBV-TP, SFU-TP, ara-ATP, and N^4-OH-CTP on the activity of *Ec*CTPS and its ability to form filaments *in vitro*. Ara-ATP was able to replace ATP as a substrate for *Ec*CTPS. Despite ara-ATP being less efficient (*i.e.*, $k_{cat}/[S]_{0.5}$) than ATP at supporting Gln- and NH_3-dependent CTP formation by ~2.5- and ~5.5-fold, respectively, these observations suggest that ara-ATP could assist in maintaining the intracellular CTP pools when employed as an antiviral agent. Similarly, SFU-TP replaced UTP as a substrate for *Ec*CTPS, albeit ~6-fold less efficient than UTP. The UTP-binding site exhibits exquisite specificity for UTP;[61] however, it appears that the enzyme can tolerate substitution at the 2′-position since 2′,2′-difluoro-dUTP is also a substrate for *Ec*CTPS.[58] Interestingly, the amination product, 4-NH_2-SFU-TP, is also a known antiviral agent.[62] Additionally, SFU-TP prevented CTP-dependent filament formation by the enzyme. RBV-TP, like GTP, served as an allosteric activator of Gln-dependent CTP formation, indicating that the carboxamide group on the pseudobase of RBV-TP is able to mimic the interaction of O6 with *Ec*CTPS to afford activation. However, the missing part of the purine structure diminished the binding affinity ~36-fold relative to GTP, resulting in the overall efficiency of activation (k_{act}/K_A) by RBV-TP being ~24-fold less than that of GTP. Possibly, the allosteric activation of CTPS by RBV-TP may account, in part, for the continued production of CTP despite the depletion of the GTP pools arising from the inhibition of IMPDH by ribavirin-5′-monophosphate. Finally, *Ec*CTPS was inhibited by the active metabolite of molnupiravir, N^4-OH-CTP, although the competitive inhibition constant was ~7.7-fold weaker than that accompanying feedback inhibition by CTP. Like, CTP, N^4-OH-CTP induced filament formation by the enzyme. Overall, these observations demonstrate that the 5′-TP metabolites of several antiviral drugs can affect the activity of CTP synthase and, consequently, may impact the level of the intracellular CTP pools. Such an impact may also have an effect on the host immune response that relies on the activation and proliferation of T cells and B cells for adaptive immunity.[10b,63] These results underscore the need to explore such effects by these and other antiviral metabolites on the human isoforms of CTPS.

Experimental Section

General. All chemicals, unless stated otherwise, were purchased from Sigma-Aldrich Canada Ltd. (Oakville, ON, Canada). GTP, ara-ATP, and RBV-TP were purchased from Jena Bioscience (Jena, Germany). SFU-TP was purchased from Toronto Research Chemicals (Toronto, ON, Canada) and Sierra Bioresearch (Tucson, AZ). β-D-2′-Deoxy-2′-α-F-2′-β-C-methyluridine was obtained from SynInnova (Edmonton, AB, Canada) and β-D-2′-Deoxy-2′-α-F-2′-β-C-methylcytidine was obtained from Toronto Research Chemicals (Toronto, ON, canada). His·Bind resin (Novagen) was purchased from EMD Millipore (San Diego, CA, USA). For HPLC experiments, a Waters 510 pump and automated gradient controller were used for solvent delivery. Injections were made using a Rheodyne 7725i sample injector fitted with a 20-μL injection loop, and a Waters 486 absorbance detector was used to detect nucleotides. Kinetic studies were conducted using an Agilent 8453 UV-vis diode array spectrophotometer. Low resolution (LR) and high resolution (HR) electrospray ionization (ESI) mass spectra (MS) were collected using a Bruker microTOF Focus orthogonal ESI-TOF mass spectrometer instrument operating in negative ion mode. ^{1}H and ^{31}P NMR spectra were obtained using a Bruker AV 500 MHz spectrometer at the Dalhousie University Nuclear Magnetic Resonance Research Resource Centre (NMR-3). Chemical shifts (δ in ppm) for ^{1}H and ^{31}P NMR spectra are reported relative to the residual solvent signal for D_2O (δ 4.79) and an external standard of 85% phosphoric acid, respectively.[64]

***N*^{4}-OH-CTP.** N^4-OH-CTP was obtained by reacting CTP with hydroxylamine following a protocol similar to that described by Painter *et al*.[57] CTP (0.137 g, 0.260 mmol) was dissolved in a solution of hydroxylamine (2.0 mL, 2.0 M, pH 5) and the pH was adjusted to 5.0 by addition of NaOH. The reaction mixture was placed in a sealed 5-mL reaction vial and heated with stirring at 55 °C for 5 h. The mixture was then cooled to room temperature and a solution of triethylammonium bicarbonate (TEAB, 100 mM, 2 mL) was added. TEAB buffer (1.0 M, pH 8.0) was prepared by bubbling CO_2(g) through a solution of triethylamine (1.0 M) for 5 h.) The reaction mixture was then subjected to anion-exchange chromatography on a DEAE-Sephadex A-25 matrix (2.5 cm i.d. × 42 cm) and eluted at a flow rate of 0.7 mL/min using a 1.5-L gradient of TEAB (0.1 – 0.5 M), followed by a 0.2-L gradient of TEAB (0.5 – 1.0 M) and 0.5 L of TEAB (1.0 M).[65] Fractions (12 mL) were collected and the absorbance of those fractions was measured at 260 nm. Fractions with elevated absorbance readings corresponding to three distinct peaks were pooled to yield three combined fractions (I – III, **Fig. S2**). Production of the hydroxamic acid was verified visually by production of a purple colour upon treatment with 1% $FeCl_3$ in 1 N HCl.[66] The solvent was removed from each of these combined fractions using rotary evaporation (≤ 37 °C). The residue was then dissolved in water and lyophilized several (~4) times until a consistent mass was obtained. The various phosphoryated derivatives of NHC in the combined fractions were identified using ESI-MS. Fraction III contained N^4-OH-CTP and the purity of the nucleotide (≥ 99%) was verified using reversed-phase HPLC on a Kinetex 5μ C18 100A column (250 × 4.6 mm, Phenomenex) using a flow rate of 1.0 mL/min and NH_4HCO_3 solution (50 mM) containing acetonitrile (10%) and (n-Bu)$_3$NH (2.0 μM), adjusted to pH 7.0 with acetic acid, as the eluant and UV detection at 260 nm. N^4-OH-CTP was

converted to its sodium salt by treatment with AG 50W-X8 (Na^+-form). The concentration of N^4-OH-CTP was determined by comparison of the integration of the H6 proton (δ 7.15) in the ^{1}H NMR spectrum with the signal arising from a pyrazine internal standard (0.80 mM, δ 8.59). Yield = 18%. ^{1}H NMR (500 MHz, D_2O) δ 7.18 (d, J = 8.3 Hz, 1H), 5.93 (d, J = 6.5 Hz, 1H), 5.81 (d, J = 8.3 Hz, 1H), 4.46 – 4.31 (m, 2H), 4.23 – 4.08 (m, 3H); ^{31}P NMR (202 MHz, D_2O) δ –10.10 (d, J = 19.4 Hz), –11.44 (d, J = 20.2 Hz), –23.13 (t, J = 19.8 Hz); HR-ESIMS m/z calcd for $C_9H_{15}N_3O_{15}P_3^-$ $[M–H]^-$: 497.9721, found 497.9725. The ^{31}P NMR spectral data were in agreement with published data.[57]

Expression and purification of recombinant *Ec*CTPS. Wild-type *Ec*CTPS was purified from *E. coli* BL21(DE3) cells transformed with the pET-15b-CTPS1 plasmid as described previously.[24b] Soluble *Ec*CTPS bearing an N-terminal His_6-tag was purified by metal ion affinity chromatography using established protocols (Novagen)[67] and dialyzed into assay buffer [HEPES (70 mM, pH 8.0) containing EGTA (0.5 mM) and $MgCl_2$ (10 mM)]. Recombinant enzyme preparations were ≥ 97% pure as determined using SDS-PAGE (10%) analysis, and the protein concentration was determined using Bradford assays conducted according to the manufacturer's directions (Bio-Rad Laboratories, Mississauga, ON) with bovine serum albumin standards. The N-terminal His_6-tag was not removed from the protein.

Enzyme assays. *Ec*CTPS activity was determined at 37 °C using a continuous spectrophotometric assay as previously described.[24b] In brief, the rate of *Ec*CTPS-catalyzed conversion of UTP to CTP was measured by following the change in absorbance at 291 nm ($\Delta\varepsilon_{291}$ = 1331 M^{-1} cm^{-1}) for 60 s. When using SFU-TP as the substrate, the change in absorbance at 282 nm was monitored ($\Delta\varepsilon_{282}$ = 4036 M^{-1} cm^{-1}, *vide infra*). Reactions were conducted in HEPES buffer (70 mM, pH 8.0) and typically contained *Ec*CTPS (4.0 – 20.0 μg/mL), EGTA (0.5 mM), $MgCl_2$ (10 mM), UTP (1.0 mM), and ATP (1.0 mM) in a total volume of 0.3 mL in a 0.2-cm quartz cuvette, unless mentioned otherwise. Enzyme and nucleotides were pre-incubated at 37 °C for 2 min followed by the addition of the ammonia source (NH_4Cl or L-Gln) to initiate the reaction. For reactions using NH_4Cl as the substrate (5.0 – 150.0 mM), KCl was used to maintain ionic strength at 0.15 M. The $[NH_3]$ present at pH 8.0 was calculated using a pKa (NH_4^+) of 9.24 (*i.e.*, $[NH_3] = 0.0575\cdot[NH_4Cl]_{total}$).[68] For reactions using Gln as the substrate (0.05 – 6.0 mM), the concentration of GTP was 0.25 mM. GTP-dependent activation assays were conducted using Gln (6.0 mM) as the substrate and varying the concentration of GTP (0.05 – 1.00 mM) with the concentrations of UTP (1.0 mM), ATP (1.0 mM), and *Ec*CTPS (4.7 μg/mL) as indicated. The kinetic parameters for UTP (0 – 3.0 mM) were obtained by following Gln-dependent CTP formation with the concentrations of GTP (0.25 mM), ATP (1.0 mM), and *Ec*CTPS (7.6 μg/mL) as indicated. The values of k_{cat} and K_m were determined by fitting eqn. 1 to initial velocity data using non-linear regression analysis with *KaleidaGraph* v. 4.02 from Synergy Software (Reading, PA).[52] Similarly, k_{cat}, $[S]_{0.5}$, and n (Hill coefficient) values for ATP, UTP, ara-ATP, and SFU-TP as substrates were determined by fitting eqn. 2 to the corresponding initial velocity data. For the activation and inhibition of *Ec*CTPS by GTP, the values of K_A, k_{act}, K_{inhib}, k_o, and n were obtained by fitting eqn. 3 to the initial velocity data. For the activation of *Ec*CTPS by RBV-TP, the values of K_A, k_{act}, and k_o were obtained by fitting eqn. 4 to the corresponding initial velocity data. All kinetic parameters were determined in triplicate and average values are reported. The reported errors are the standard deviations.

$$\frac{v_i}{[E]_T} = \frac{k_{cat}[S]}{K_m + [S]} \quad (1)$$

$$\frac{v_i}{[E]_T} = \frac{k_{cat}[S]^n}{[S]^n_{0.5} + [S]^n} \quad (2)$$

$$\frac{v_i}{[E]_T} = \frac{k_o + \left(\frac{k_{act}[A]}{K_A}\right)}{1 + \frac{[A]}{K_A} + \left(\frac{[A]}{K_{inhib}}\right)^n} \quad (3)$$

$$\frac{v_i}{[E]_T} = \frac{k_o + \left(\frac{k_{act}[A]}{K_A}\right)}{1 + \frac{[A]}{K_A}} \quad (4)$$

IC_{50} values for the inhibition of *Ec*CTPS by CTP and N^4-OH-CTP were determined by following the Gln-dependent formation of CTP from UTP (either 50 μM or 200 μM) in the presence of Gln (6.0 mM), ATP (1.0 mM), and increasing concentrations of CTP or N^4-OH-CTP. IC_{50} values were determined by fitting initial velocities to eqn. 5, where v_o and v_i correspond to the velocities observed in the absence and presence of inhibitor, respectively. Furthermore, initial velocities were measured in the presence of fixed concentrations of CTP (0, 0.06, 0.12, and 0.18 mM) and N^4-OH-CTP (0, 0.60, 1.20, and 1.80 mM) and apparent $[S]_{0.5}/V_{max}$ values, obtained from non-linear regression analysis of the Michaelis-Menten plots, were replotted against concentration of inhibitor to estimate the value of the competitive inhibition constant (K_i) in accord with eqn. 6. K_i determinations with N^4-OH-CTP were conducted using a 0.1-cm quartz cuvette.

$$\frac{v_i}{v_o} = \frac{IC_{50}^n}{IC_{50}^n + [I]^n} \quad (5)$$

$$\frac{v_i}{[E]_T} = \frac{k_{cat}[S]}{[S]_{0.5}\left(1 + \frac{[I]}{K_i}\right) + [S]} \quad (6)$$

SFU-TP-dependent UV assay. Although ΔA_{291} could be used to monitor *Ec*CTPS activity with SFU-TP, the difference in extinction coefficients between SFU-TP and 4-NH_2-SFU-TP was greater at 282 nm. To estimate the ΔA_{282} value for the triphosphates, the extinction coefficients for β-D-2′-deoxy-2′-α-F-2′-β-C-methyluridine (PSI-6206) and β-D-2′-deoxy-2′-α-F-2′-β-C-methylcytidine (PSI-6130) were determined to be 1858 ± 411 M^{-1} cm^{-1} and 5894 ± 275 M^{-1} cm^{-1}, respectively, by measuring the absorbance at 282 nm of solutions of the nucleosides (50.0, 75.0, 100.0, and 150.0 μM) in assay buffer and using the Beer-Lambert law (**Fig. S13**). Kinetic parameters for *Ec*CTPS-catalyzed turnover of SFU-TP were therefore determined using UV spectrophotometry by following the change in absorbance at 282 nm ($\Delta\varepsilon_{282}$ = 4036 ± 494 $M^{-1}cm^{-1}$).

Gln-dependent amination of SFU-TP was measured using saturating conditions of Gln (6.0 mM) and ATP (1.0 mM), and varying amounts of SFU-TP (0.025 – 1.000 mM). GTP was maintained at a fixed saturating concentration of 0.25 mM in all assays with varying concentrations of SFU-TP. Additionally, Gln-dependent amination of SFU-TP was measured at fixed concentrations of SFU-TP (1.0 mM) and ATP (1.0 mM), and varying amounts of Gln (0.05 – 10.00 mM). Eqn. 1 was fitted to the initial velocity data when Gln was the variable substrate and eqn. 2 was fitted to the initial velocity data when SFU-TP was the

variable substrate. Non-linear regression analysis was used to determine values of k_{cat}, K_m, $[S]_{0.5}$, and n. Unfortunately, the cost of SFU-TP precluded detailed examination of the less physiologically relevant NH_3-dependent amination.

Product analysis of enzymatically prepared 4-NH_2-SFU-TP. To confirm the *Ec*CTPS-catalyzed conversion of SFU-TP to 4-NH_2-SFU-TP, SFU-TP (2.0 mM) was incubated at 37 °C in assay buffer containing *Ec*CTPS (0.5 μM) in the presence of ATP (1.0 mM) and NH_4Cl (150 mM) in a total volume of 1.0 mL. NH_4Cl was used as the substrate rather than Gln to avoid the presence of an added nucleotide (*i.e.*, GTP) in the analysis. At 0, 5, 15, 30, 60, 120, and 180 min, aliquots (100 μL) were removed, and the enzyme was removed by centrifugation through a 10-kDa MWCO spin-filter (Millipore). The flow-through samples were analyzed using LRESI-MS.

Electron microscopy. The ability of nucleotide analogues to induce or disrupt filament formation by *Ec*CTPS was assessed by TEM using a protocol similar to those described previously.[21b,39c] *Ec*CTPS (15 μM) was incubated in HEPES (assay) buffer (70 mM, pH 8.0) containing EGTA (0.5 mM), $MgCl_2$ (10 mM), and either GTP (1.0 mM), RBV-TP (1.0 mM), SFU-TP (1.0 mM or 5.0 mM) or N^4-OH-CTP (1.0 mM) in the absence or presence of CTP (1.0 mM) for 30 min at 37 °C. Samples were diluted 10-fold using assay buffer containing 50% glycerol before being deposited on Formvar-coated carbon grids (TAAB Laboratories, Berkshire, UK) for uranyl acetate (0.7%) staining. Negative stain transmission electron micrographs were obtained using a JEOL 1230 transmission electron microscope.

Acknowledgements

We thank Mary Ann Trevors of the Dalhousie Faculty of Medicine Electron Microscopy Facility for her assistance with TEM experiments. This work was supported by an operating grant from the Nova Scotia COVID-19 Health Research Coalition (NSHA Research & Innovation (Nova Scotia Health), Dalhousie University, Dalhousie Medical Research Foundation, the QEII Health Sciences Centre Foundation, the IWK Foundation, the IWK Health Centre, the Dartmouth General Hospital Foundation, and Research Nova Scotia) (S.L.B.), a MITACS Research Training Grant (T.D.G.), and the NSERC CREATE Training Program in BioActives (510963).

Keywords: CTP synthase • antiviral • inhibition kinetics • activation • filaments

[1] a) Y. A. Helmy, M. Fawzy, A. Elaswad, A. Sobieh, S. P. Kenney, A. A. Shehata, *J. Clin. Med.* **2020**, *9*(4), 1225; b) R. Lu, X. Zhao, J. Li, P. Niu, B. Yang, H. Wu, W. Wang, H. Song, B. Huang, N. Zhu, Y. Bi, X. Ma, F. Zhan, L. Wang, T. Hu, H. Zhou, Z. Hu, W. Zhou, L. Zhao, J. Chen, Y. Meng, J. Wang, Y. Lin, J. Yuan, Z. Xie, J. Ma, W. J. Liu, D. Wang, W. Xu, E. C. Holmes, G. F. Gao, G. Wu, W. Chen, W. Shi, W. Tan, *Lancet* **2020**, *395*(10224), 565-574; c) N. Zhu, D. Zhang, W. Wang, X. Li, B. Yang, J. Song, X. Zhao, B. Huang, W. Shi, R. Lu, P. Niu, F. Zhan, X. Ma, D. Wang, W. Xu, G. Wu, G. F. Gao, W. Tan, *New Engl. J. Med.* **2020**, *382*(8), 727-733.

[2] J. Y. Li, Z. You, Q. Wang, Z. J. Zhou, Y. Qiu, R. Luo, X. Y. Ge, *Microbes Infect.* **2020**, *22*(2), 80-85.

[3] a) P. O. Smith, P. Jin, K. M. Rahman, *Curr. Res. Pharmacol. Drug Discov.* **2022**, *3*, 100072; b) T. U. Singh, S. Parida, M. C. Lingaraju, M. Kesavan, D. Kumar, R. K. Singh, *Pharmacol. Rep.* **2020**, *72*(6), 1479-1508; c) R. A. Al-Horani, S. Kar, *Viruses* **2020**, *12*(10), 1092.

[4] H. Li, Y. Zhou, M. Zhang, H. Wang, Q. Zhao, J. Liu, *Antimicrob. Agents Chemother.* **2020**, AAC.00483-00420.

[5] a) J. H. Beigel, K. M. Tomashek, L. E. Dodd, A. K. Mehta, B. S. Zingman, A. C. Kalil, E. Hohmann, H. Y. Chu, A. Luetkemeyer, S. Kline, D. Lopez de Castilla, R. W. Finberg, K. Dierberg, V. Tapson, L. Hsieh, T. F. Patterson, R. Paredes, D. A. Sweeney, W. R. Short, G. Touloumi, D. C. Lye, N. Ohmagari, M. D. Oh, G. M. Ruiz-Palacios, T. Benfield, G. Fätkenheuer, M. G. Kortepeter, R. L. Atmar, C. B. Creech, J. Lundgren, A. G. Babiker, S. Pett, J. D. Neaton, T. H. Burgess, T. Bonnett, M. Green, M. Makowski, A. Osinusi, S. Nayak, H. C. Lane, A.-S. G. Members, *New Engl. J. Med.* **2020**, *383*(19), 1813-1826; b) M. Wang, R. Cao, L. Zhang, X. Yang, J. Liu, M. Xu, Z. Shi, Z. Hu, W. Zhong, G. Xiao, *Cell Res.* **2020**, *30*(3), 269-271; c) D. Siegel, H. C. Hui, E. Doerffler, M. O. Clarke, K. Chun, L. Zhang, S. Neville, E. Carra, W. Lew, B. Ross, Q. Wang, L. Wolfe, R. Jordan, V. Soloveva, J. Knox, J. Perry, M. Perron, K. M. Stray, O. Barauskas, J. Y. Feng, Y. Xu, G. Lee, A. L. Rheingold, A. S. Ray, R. Bannister, R. Strickley, S. Swaminathan, W. A. Lee, S. Bavari, T. Cihlar, M. K. Lo, T. K. Warren, R. L. Mackman, *J. Med. Chem.* **2017**, *60*(5), 1648-1661.

[6] F. Pourkarim, S. Pourtaghi-Anvarian, H. Rezaee, *Pharmacol. Res. Perspect.* **2022**, *10*(1), e00909.

[7] a) M. L. Agostini, E. L. Andres, A. C. Sims, R. L. Graham, T. P. Sheahan, X. Lu, E. C. Smith, J. B. Case, J. Y. Feng, R. Jordan, A. S. Ray, T. Cihlar, D. Siegel, R. L. Mackman, M. O. Clarke, R. S. Baric, M. R. Denison, *mBio* **2018**, *9*(2), e00221-00218; b) C. J. Gordon, E. P. Tchesnokov, E. Woolner, J. K. Perry, J. Y. Feng, D. P. Porter, M. Götte, *J. Biol. Chem.* **2020**, *295*(20), 6785-6797.

[8] H. Vatandaslar, *Int. J. Mol. Sci.* **2022**, *23*(15), 8302.

[9] a) J.-J. Yoon, M. Toots, S. Lee, M. E. Lee, B. Ludeke, J. M. Luczo, K. Ganti, R. M. Cox, Z. M. Sticher, V. Edpuganti, D. G. Mitchell, M. A. Lockwood, A. A. Kolykhalov, A. L. Greninger, M. L. Moore, G. R. Painter, A. C. Lowen, S. M. Tompkins, R. Fearns, M. G. Natchus, R. K. Plemper, *Antimicrob. Agents Chemother.* **2018**, *62*(8), e00766-00718; b) M. Toots, J. J. Yoon, R. M. Cox, M. Hart, Z. M. Sticher, N. Makhsous, R. Plesker, A. H. Barrena, P. G. Reddy, D. G. Mitchell, R. C. Shean, G. R. Bluemling, A. A. Kolykhalov, A. L. Greninger, M. G. Natchus, G. R. Painter, R. K. Plemper, *Sci. Transl. Med.* **2019**, *11*(515), eaax5866; c) M. L. Agostini, A. J. Pruijssers, J. D. Chappell, J. Gribble, X. Lu, E. L. Andres, G. R. Bluemling, M. A. Lockwood, T. P. Sheahan, A. C. Sims, M. G. Natchus, M. Saindane, A. A. Kolykhalov, G. R. Painter, R. S. Baric, M. R. Denison, *J. Virol.* **2019**, *93*(24), e01348-01319; d) T. P. Sheahan, A. C. Sims, S. Zhou, R. L. Graham, A. J. Pruijssers, M. L. Agostini, S. R. Leist, A. Schäfer, K. H. Dinnon, L. J. Stevens, J. D. Chappell, X. Lu, T. M. Hughes, A. S. George, C. S. Hill, S. A. Montgomery, A. J. Brown, G. R. Bluemling, M. G. Natchus, M. Saindane, A. A. Kolykhalov, G. Painter, J. Harcourt, A. Tamin, N. J. Thornburg, R. Swanstrom, M. R. Denison, R. S. Baric, *Sci. Transl. Med.* **2020**, *12*, eabb5883; e) C. J. Gordon, E. P. Tchesnokov, R. F. Schinazi, M. Götte, *J. Biol. Chem.* **2021**, *297*(1), 100770.

[10] a) K. M. Stegmann, A. Dickmanns, N. Heinen, C. Blaurock, T. Karrasch, A. Breithaupt, R. Klopfleisch, N. Uhlig, V. Eberlein, L. Issmail, S. T. Herrmann, A. Schreieck, E. Peelen, H. Kohlhof, B. Sadeghi, A. Riek, J. R. Speakman, U. Groß, D. Görlich, D. Vitt, T. Müller, T. Grunwald, S. Pfaender, A. Balkema-Buschmann, M. Dobbelstein, *iScience* **2022**, *25*(5), 104293; b) C. Qin, Y. Rao, H. Yuan, T. Y. Wang, J. Zhao, B. Espinosa, Y. Liu, S. Zhang, A. C. Savas, Q. Liu, M. Zarinfar, S. Rice, J. Henley, L. Comai, N. A. Graham, C. Chen, C. Zhang, P. Feng, *Proc. Natl. Acad. Sci. U.S.A.* **2022**, *119*(26), e2122897119; c) J. F. Demarest, M. Kienle, R. Boytz, M. Ayres, E. J. Kim, J. J. Patten, D. Chung, V. Gandhi, R. A. Davey, D. B. Sykes, N. Shohdy, J. C. Pottage, V. S. Kumar, *Antiviral Res.* **2022**, *206*, 105403.

[11] a) A. Danchin, P. Marlière, *Environ. Microbiol.* **2020**, *22*(6), 1977-1985; b) Z. Ou, C. Ouzounis, D. Wang, W. Sun, J. Li, W. Chen, P. Marlière, A. Danchin, *Genome Biol. Evol.* **2020**, *12*(12), 2467-2485; c) N. Cluzel, A. Lambert, Y. Maday, G. Turinici, A. Danchin, *C. R. Biol.* **2020**, *343*(2), 177-209.

[12] S. Hatse, E. De Clercq, J. Balzarini, *Biochem. Pharmacol.* **1999**, *58*(4), 539-555.

[13] a) M. Bakovic, M. D. Fullerton, V. Michel, *Biochem. Cell Biol.* **2007**, *85*(3), 283-300; b) D. B. Ostrander, D. J. O'Brien, J. A. Gorman, G. M. Carman, *J. Biol. Chem.* **1998**, *273*(30), 18992-19001.

[14] K. Wellner, H. Betat, M. Mörl, *Biochim. Biophys. Acta Gene Regul. Mech.* **2018**, *1861*(4), 433-441.

[15] P. Shridas, C. J. Waechter, *J. Biol. Chem.* **2006**, *281*(42), 31696-31704.

[16] E. E. Rivera-Serrano, A. S. Gizzi, J. J. Arnold, T. L. Grove, S. C. Almo, C. E. Cameron, *Ann. Rev. Virol.* **2020**, *7*(1), 421-446.

[17] a) H. Zalkin, *Adv. Enzymol. Relat. Areas Mol. Biol.* **1993**, *66*, 203-309; b) C. J. van Moorsel, A. M. Bergman, G. Veerman, D. A. Voorn, V. W. Ruiz van Haperen, J. R. Kroep, H. M. Pinedo, G. J. Peters, *Biochim. Biophys. Acta* **2000**, *1474*(1), 5-12.

[18] a) I. Lieberman, *J. Biol. Chem.* **1956**, *222*, 765-775; b) H. Kizaki, T. Sakurada, G. Weber, *Biochim. Biophys. Acta* **1981**, *662*(1), 48-54; c) J. G. Robertson, J. J. Villafranca, *Biochemistry* **1993**, *32*(14), 3769-3777.

[19] a) C. W. Long, A. B. Pardee, *J. Biol. Chem.* **1967**, *242*(20), 4715-4721; b) A. Levitzki, D. E. Koshland, Jr., *Proc. Natl. Acad. Sci. U S A* **1969**, *62*(4), 1121-1128; c) A. Levitzki, D. E. Koshland, Jr., *Biochemistry* **1972**, *11*(2), 247-253.

[20] A. Pappas, W. L. Yang, T. S. Park, G. M. Carman, *J. Biol. Chem.* **1998**, *273*(26), 15954-15960.

[21] a) I. Lauritsen, M. Willemoës, K. F. Jensen, E. Johansson, P. Harris, *Acta Crystallogr.* **2011**, *F67*(Pt 2), 201-208; b) R. M. Barry, A. F. Bitbol, A. Lorestani, E. J. Charles, C. H. Habrian, J. M. Hansen, H. J. Li, E. P. Baldwin, N. S. Wingreen, J. M. Kollman, Z. Gitai, *eLife* **2014**, *3*, e03638; c) E. M. Lynch, D. R. Hicks, M. Shepherd, J. A. Endrizzi, A. Maker, J. M. Hansen, R. M. Barry, Z. Gitai, E. P. Baldwin, J. M. Kollman, *Nat. Struct. Biol.* **2017**, *24*(6), 507-514.

[22] E. M. Lynch, J. M. Kollman, *Nat. Struct. Mol. Biol.* **2020**, *27*(1), 42-48.

[23] X. Zhou, C. J. Guo, H. H. Hu, J. Zhong, Q. Sun, D. Liu, S. Zhou, C. C. Chang, J. L. Liu, *J. Genet. Genomics* **2019**, *46*(11), 537-545.

[24] a) A. Levitzki, D. E. Koshland, Jr., *Biochemistry* **1972**, *11*(2), 241-246; b) S. L. Bearne, O. Hekmat, J. E. MacDonnell, *Biochem. J.* **2001**, *356*(Pt 1), 223-232; c) M. Willemoës, *Arch. Biochem. Biophys.* **2004**, *424*, 105-111; d) G. D. McCluskey, S. L. Bearne, *Biochim. Biophys. Acta Gen. Subj.* **2018**, *1862*(12), 2714-2727; e) S. L. Bearne, C.-J. Guo, J.-L. Liu, *Biomolecules* **2022**, *12*(5), 647.

[25] a) G. J. Kang, D. A. Cooney, J. D. Moyer, J. A. Kelley, H. Y. Kim, V. E. Marquez, D. G. Johns, *J. Biol. Chem.* **1989**, *264*(2), 713-718; b) K. J. Schimmel, H. Gelderblom, H. J. Guchelaar, *Curr. Cancer Drug Targets* **2007**, *7*(5), 504-509.

[26] E. De Clercq, *Adv. Virus. Res.* **1993**, *42*, 1-55.

[27] a) W. Y. Gao, D. G. Johns, H. Mitsuya, *Nucleosides Nucleotides Nucleic Acids* **2000**, *19*(1-2), 371-377; b) N. Dereuddre-Bosquet, B. Roy, K. Routledge, P. Clayette, G. Foucault, M. Lepoivre, *Antiviral Res.* **2004**, *61*, 67-70.

[28] Y. Li, H.-X. Zhang, W.-D. Luo, C. W. K. Lam, C.-Y. Wang, L.-P. Bai, V. K. W. Wong, W. Zhang, Z.-H. Jiang, *Front. Pharmacol.* **2021**, *12*, 647280.

[29] a) J. A. Endrizzi, H. Kim, P. M. Anderson, E. P. Baldwin, *Biochemistry* **2004**, *43*(21), 6447-6463; b) J. A. Endrizzi, H. Kim, P. M. Anderson, E. P. Baldwin, *Biochemistry* **2005**, *44*(41), 13491-13499; c) P. Kursula, S. Flodin, M. Ehn, M. Hammarstrom, H. Schuler, P. Nordlund, *Acta Crystallograph. Sect. F Struct. Biol. Cryst. Commun.* **2006**, *62*(Pt 7), 613-617.

[30] P. Prusiner, M. Sundaralingam, *Nat. New Biol.* **1973**, *244*(134), 116-118.

[31] A. A. Elfiky, *Life Sci.* **2020**, *253*, 117592.

[32] a) S. Tong, Y. Su, Y. Yu, C. Wu, J. Chen, S. Wang, J. Jiang, *Int. J. Antimicrob. Agents* **2020**, *56*(3), 106114; b) J. S. Khalili, H. Zhu, N. S. A. Mak, Y. Yan, Y. Zhu, *J. Med. Virol.* **2020**, *92*(7), 740-746; c) I. F. Hung, K. C. Lung, E. Y. Tso, R. Liu, T. W. Chung, M. Y. Chu, Y. Y. Ng, J. Lo, J. Chan, A. R. Tam, H. P. Shum, V. Chan, A. K. Wu, K. M. Sin, W. S. Leung, W. L. Law, D. C. Lung, S. Sin, P. Yeung, C. C. Yip, R. R. Zhang, A. Y. Fung, E. Y. Yan, K. H. Leung, J. D. Ip, A. W. Chu, W. M. Chan, A. C. Ng, R. Lee, K. Fung, A. Yeung, T. C. Wu, J. W. Chan, W. W. Yan, W. M. Chan, J. F. Chan, A. K. Lie, O. T. Tsang, V. C. Cheng, T. L. Que, C. S. Lau, K. H. Chan, K. K. To, K. Y. Yuen, *Lancet* **2020**, *395*(10238), 1695-1704; d) X. Xie, A. E. Muruato, X. Zhang, K. G. Lokugamage, C. R. Fontes-Garfias, J. Zou, J. Liu, P. Ren, M. Balakrishnan, T. Cihlar, C. K. Tseng, S. Makino, V. D. Menachery, J. P. Bilello, P. Y. Shi, *Nat. Commun.* **2020**, *11*(1), 5214; e) H. Li, N. Xiong, C. Li, Y. Gong, L. Liu, H. Yang, X. Tan, N. Jiang, Q. Zong, J. Wang, Z. Lu, X. Yin, *Int. J. Infect. Dis.* **2021**, doi.org/10.1016/j.ijid.2021.1001.1055; f) N. Borbone, G. Piccialli, G. N. Roviello, G. Oliviero, *Molecules* **2021**, *26*(4), 986.

[33] J. D. Graci, C. E. Cameron, *Rev. Med. Virol.* **2006**, *16*(1), 37-48.

[34] a) T. P. Zimmerman, R. D. Deeprose, *Biochem. Pharmacol.* **1978**, *27*(5), 709-716; b) T. Page, J. D. Connor, *Int. J. Biochem.* **1990**, *22*(4), 379-383.

[35] P. W. Hager, F. R. Collart, E. Huberman, B. S. Mitchell, *Biochem. Pharmacol.* **1995**, *49*(9), 1323-1329.

[36] S. K. Wray, B. E. Gilbert, M. W. Noall, V. Knight, *Antiviral Res.* **1985**, *5*(1), 29-37.

[37] W. E. Müller, A. Maidhof, H. Taschner, R. K. Zahn, *Biochem. Pharmacol.* **1977**, *26*(11), 1071-1075.

[38] F. A. Lunn, J. E. MacDonnell, S. L. Bearne, *J. Biol. Chem.* **2008**, *283*(4), 2010-2020.

[39] a) M. Ingerson-Mahar, A. Briegel, J. N. Werner, G. J. Jensen, Z. Gitai, *Nat. Cell Biol.* **2010**, *12*(8), 739-746; b) C. Noree, B. K. Sato, R. M. Broyer, J. E. Wilhelm, *J. Cell Biol.* **2010**, *190*(4), 541-551; c) G. D. McCluskey, S. L. Bearne, *J. Mol. Biol.* **2018**, *430*(8), 1201-1217.

[40] S. W. Mueller, T. H. Kiser, T. Morrisette, M. R. Zamora, D. M. Lyu, J. J. Kiser, *Transpl. Infect. Dis.* **2021**, *23*(1), e13464.

[41] S. Stridh, *Arch. Virol.* **1983**, *77*(2-4), 223-229.

[42] a) S. A. Coggins, B. Mahboubi, R. F. Schinazi, K. B., *J. Biol. Chem.* **2020**, *295*(39), 13432-13443; b) T. W. Traut, *Mol Cell Biochem* **1994**, *140*(1), 1-22.

[43] a) G. Li, E. De Clercq, *Nat. Rev. Drug Discov.* **2020**, *19*(3), 149-150; b) J. Ju, X. Li, S. Kumar, S. Jockusch, M. Chien, C. Tao, I. Morozova, S. Kalachikov, R. N. Kirchdoerfer, J. J. Russo, *Pharmacol. Res. Perspect.* **2020**, *8*(6), e00674; c) A. A. Elfiky, *Life Sci.* **2020**, *248*, 117477; d) R. Jácome, J. A. Campillo-Balderas, S. Ponce de León, A. Becerra, A. Lazcano, *Sci. Rep.* **2020**, *10*(1), 9294; e) L. Buonaguro, F. M. Buonaguro, *Infect. Agent. Cancer* **2020**, *15*, 32.

[44] a) M. Chien, T. K. Anderson, S. Jockusch, C. Tao, X. Li, S. Kumar, J. J. Russo, R. N. Kirchdoerfer, J. Ju, *J. Proteome Res.* **2020**, *19*(11), 4690-4697; b) S. Jockusch, C. Tao, X. Li, M. Chien, S. Kumar, I. Morozova, S. Kalachikov, J. J. Russo, J. Ju, *Sci. Rep.* **2020**, *10*(1), 16577; c) C. Yuan, E. C. Goonetilleke, I. C. Unarta, X. Huang, *Phys. Chem. Chem. Phys.* **2021**, *23*(36), 20117-20128.

[45] K. Zandi, F. Amblard, K. Musall, J. Downs-Bowen, R. Kleinbard, A. Oo, D. Cao, B. Liang, O. O. Russell, T. McBrayer, L. Bassit, B. Kim, R. F. Schinazi, *Antimicrob. Agents Chemother.* **2021**, *65*(1), e01652-01620.

[46] Y. S. Lim, L. P. Nguyen, G. H. Lee, S. G. Lee, K. S. Lyoo, B. Kim, S. B. Hwang, *Mol. Cells* **2021**, *44*(9), 688-695.

[47] a) H.-T. Chan, C.-M. Chao, C.-C. Lai, *J. Infect.* **2020**, *8*(58), S0163-4453; b) A. Sadeghi, A. Ali Asgari, A. Norouzi, Z. Kheiri, A. Anushirvani, M. Montazeri, H. Hosamirudsai, S. Afhami, E. Akbarpour, R. Aliannejad, A. R. Radmard, A. H. Davarpanah, J. Levi, H. Wentzel, A. Qavi, A. Garratt, B. Simmons, A. Hill, S. Merat, *J. Antomicrob. Chemother.* **2020**, *75*(11), 3379-3385.

[48] G. M. Abraham, L. Spooner, *Clin. Infect. Dis.* **2014**, *59*(3), 411-415.

[49] D. Babusis, M. P. Curry, B. Kirby, Y. Park, E. Murakami, T. Wang, A. Mathias, N. Afdhal, J. G. McHutchison, A. S. Ray, *Antimicrob. Agents Chemother.* **2018**, *62*(5), e02587-02517.

[50] M. Prajapat, N. Shekhar, P. Sarma, P. Avti, S. Singh, H. Kaur, A. Bhattacharyya, S. Kumar, S. Sharma, A. Prakash, B. Medhi, *J. Mol. Graph. Model.* **2020**, *101*, 107716.

[51] H. Zhang, K. M. Saravanan, Y. Yang, M. T. Hossain, J. Li, X. Ren, Y. Pan, Y. Wei, *Interdiscip. Sci.* **2020**, *12*(3), 368-376.

[52] I. H. Segel, *Enzyme Kinetics*, John Wiley and Sons, Inc., New York, **1975**.

[53] T. J. MacLeod, F. A. Lunn, S. L. Bearne, *Biochim. Biophys. Acta* **2006**, *1764*, 199-210.

[54] L. Tian, Z. Pang, M. Li, F. Lou, X. An, S. Zhu, L. Song, Y. Tong, H. Fan, J. Fan, *Front. Immunol.* **2022**, *13*, 855496.

[55] a) K. Negishi, C. Harada, Y. Ohara, K. Oohara, N. Nitta, H. Hayatsu, *Nucleic Acids Res.* **1983**, *11*(15), 5223-5233; b) L. J. Stuyver, T. Whitaker, T. R. McBrayer, B. I. Hernandez-Santiago, S. Lostia, P. M. Tharnish, M. Ramesh, C. K. Chu, R. Jordan, J. Shi, S. Rachakonda, K.

A. Watanabe, M. J. Otto, R. F. Schinazi, *Antimicrob. Agents Chemother.* **2003**, *47*(1), 244-254; c) S. Zhou, C. S. Hill, S. Sarkar, L. V. Tse, B. M. D. Woodburn, R. F. Schinazi, T. P. Sheahan, R. S. Baric, M. T. Heise, R. Swanstrom, *J. Infect. Dis.* **2021**, *224*(3), 415-419.

[56] F. Kabinger, C. Stiller, J. Schmitzová, C. Dienemann, G. Kokic, H. S. Hillen, C. Höbartner, P. Cramer, *Nat. Struct. Mol. Biol.* **2021**, *28*(9), 740-746.

[57] G. R. Painter, D. B. Guthrie, G. R. Bluemling, M. G. Natchus, Preparation of N^4-hydroxycytidine and derivatives and antiviral uses related thereto, Pat. no.: WO 2016106050 A1 20160630, **2016**.

[58] G. D. McCluskey, S. Mohamady, S. D. Taylor, S. L. Bearne, *ChemBioChem* **2016**, *17*, 2240-2249.

[59] a) G. R. Painter, R. A. Bowen, G. R. Bluemling, J. DeBergh, V. Edpuganti, P. R. Gruddanti, D. B. Guthrie, M. Hager, D. L. Kuiper, M. A. Lockwood, D. G. Mitchell, M. G. Natchus, Z. M. Sticher, A. A. Kolykhalov, *Antiviral Res.* **2019**, *171*, 104597; b) N. Urakova, V. Kuznetsova, D. K. Crossman, A. Sokratian, D. B. Guthrie, A. A. Kolykhalov, M. A. Lockwood, M. G. Natchus, M. R. Crowley, G. R. Painter, E. I. Frolova, I. Frolov, *J. Virol.* **2018**, *92*(3), e01965-01917.

[60] K. Nakamura, K. Fujimoto, C. Hasegawa, I. Aoki, H. Yoshitsugu, H. Ugai, N. Yatsuzuka, Y. Tanaka, K. Furihata, B. M. Maas, P. K. Wickremasingha, K. E. Duncan, M. Iwamoto, S. A. Stoch, N. Uemura, *Clin. Transl. Sci.* **2022**, *in press*.

[61] K. H. Scheit, H. J. Linke, *Eur. J. Biochem.* **1982**, *126*(1), 57-60.

[62] a) H. Ma, W. R. Jiang, N. Robledo, V. Leveque, S. Ali, T. Lara-Jaime, M. Masjedizadeh, D. B. Smith, N. Cammack, K. Klumpp, J. Symons, *J. Biol. Chem.* **2007**, *282*(41), 29812-29820; b) E. Murakami, H. Bao, M. Ramesh, T. R. McBrayer, T. Whitaker, H. M. Micolochick Steuer, R. F. Schinazi, L. J. Stuyver, A. Obikhod, M. J. Otto, P. A. Furman, *Antimicrob. Agents Chemother.* **2007**, *51*(2), 503-509; c) E. Murakami, C. Niu, H. Bao, H. M. Micolochick Steuer, T. Whitaker, T. Nachman, M. A. Sofia, P. Wang, M. J. Otto, P. A. Furman, *Antimicrob. Agents Chemother.* **2008**, *52*(2), 458-464.

[63] E. M. Lynch, M. A. DiMattia, S. Albanese, G. C. P. van Zundert, J. M. Hansen, J. D. Quispe, M. A. Kennedy, A. Verras, K. Borrelli, A. V. Toms, N. Kaila, K. D. Kreutter, J. J. McElwee, J. M. Kollman, *Proc. Natl. Acad. Sci. U.S.A.* **2021**, *118*(40), e2107968118.

[64] H. E. Gottlieb, V. Kotlyar, A. Nudelman, *J. Org. Chem.* **1997**, *62*, 7512-7515.

[65] J. Greenhut, F. B. Rudolph, *J. Chromatogr. A* **1985**, *319*, 461-466.

[66] R. M. Reeve, *Stain Technol.* **1959**, *34*(4), 209-211.

[67] Novagen, *pET System Manual, 7th ed., TB055* **1997**, 18-64.

[68] A. Iyengar, S. L. Bearne, *Biochem. J.* **2003**, *369*(Pt 3), 497-507.

Entry for the Table of Contents

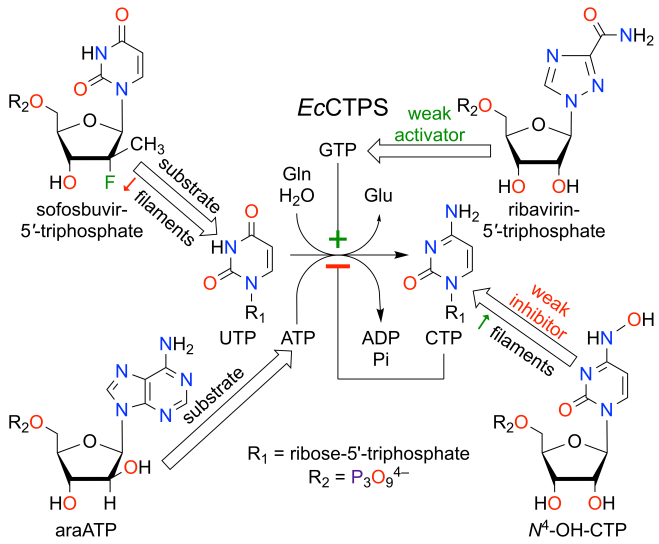

The repurposing of antiviral drugs may afford therapies to counter pandemics such as COVID-19. Viral replication is sensitive to intracellular CTP levels, yet little is known about the effects of antiviral drug metabolites on CTP synthase activity. We show that the 5′-triphosphates of several antiviral drugs can act as substrates, activators, or inhibitors of the enzyme, underscoring the need to explore such effects.